

# Transient Process of Dissipative Soliton Generation in Normal Dispersion Fiber Lasers

Ge Yanqi<sup>1,2</sup> Luo Jiaolin<sup>1,2</sup> Zhang Shumin<sup>3</sup> Tang Dingyuan<sup>1,2</sup>  
Shen Deyuan<sup>4</sup> Zhao Luming<sup>1,2</sup>

<sup>1</sup> Jiangsu Key Laboratory of Advanced Laser Materials and Devices, Jiangsu Normal University,  
Xuzhou, Jiangsu 221116, China  
<sup>2</sup> School of Physics and Electronic Engineering, Jiangsu Normal University,  
Xuzhou, Jiangsu 221116, China  
<sup>3</sup> College of Physics Science and Information Engineering, Hebei Advanced Thin Films Laboratory,  
Hebei Normal University, Shijiazhuang, Hebei 050024, China  
<sup>4</sup> Department of Optical Science and Engineering, Fudan University, Shanghai 200433, China

**Abstract** The transient process of dissipative soliton (DS) generation is numerically revealed in normal dispersion fiber lasers. It is shown that the gain dispersion is critical for the DS generation. The steep spectral edges of DSs are the consequence of the interaction among the normal dispersion, fiber nonlinearity, gain and loss, and gain dispersion effect. Narrow gain bandwidth could result in multiple DSs while broad gain bandwidth (up to 100 nm) could support DS generation provided that enough pump power is available. Consequently, DSs could be generated in fiber lasers even when the gain bandwidth is broad and there is no requirement for other spectral filtering in cavity.

**Key words** nonlinear optics; transient process; dissipative solitons; fiber lasers; normal dispersion; gain dispersion

**OCIS codes** 190.5530; 140.3510

## 正色散光纤激光器中耗散孤子形成的瞬态过程

葛颜绮<sup>1,2</sup> 罗娇林<sup>1,2</sup> 张书敏<sup>3</sup> 唐定远<sup>1,2</sup> 沈德元<sup>4</sup> 赵鹭明<sup>1,2</sup>

<sup>1</sup> 江苏师范大学江苏省先进激光材料与器件重点实验室, 江苏 徐州 221116  
<sup>2</sup> 江苏师范大学物理与电子工程学院, 江苏 徐州 221116  
<sup>3</sup> 河北师范大学物理科学与信息工程学院, 河北省新型薄膜材料实验室, 河北 石家庄 050024  
<sup>4</sup> 复旦大学光科学与工程系, 上海 200433

**摘要** 对正色散光纤激光器中耗散孤子的形成过程进行了数值模拟。数值模拟结果表明增益色散对耗散孤子的形成起决定性作用。耗散孤子的陡峭光谱边缘是正色散效应、光纤非线性效应、增益和损耗以及增益色散效应之间共同作用的结果。窄增益带宽可以导致多个耗散孤子的形成,与此同时,宽的增益带宽(以 100 nm 为例)在抽运强度足够的条件下可以支持耗散孤子的形成。即使激光腔内不存在其他光谱限制效应,耗散孤子仍可以在具有宽增益带宽的光纤激光器中形成。

**关键词** 非线性光学;瞬态过程;耗散孤子;光纤激光器;正色散;增益色散

**中图分类号** O437 **文献标识码** A **doi**: 10.3788/CJL201340.1005006

### 1 Introduction

Due to the intrinsic features of an ultrashort pulse, various applications are expected; measurement of

ultrafast phenomena using the short pulse width, bio-microscopy using the high peak power, optical coherent tomography using the broad spectrum, and so on. Both

收稿日期: 2013-05-29; 收到修改稿日期: 2013-06-14

基金项目: 国家自然科学基金(61275109)、江苏高校优势学科建设工程、江苏师范大学研究生科研创新计划

作者简介: 葛颜绮(1987—),女,硕士研究生,主要从事锁模光纤激光器方面的研究。E-mail: 14744431@qq.com

导师简介: 赵鹭明(1976—),男,博士,教授,主要从事锁模光纤激光器、光纤放大器、光孤子动力学等方面的研究。

E-mail: zhaoluming@jsnu.edu.cn(通信联系人)

solid-state lasers and fiber lasers can be the ultrashort pulse sources. Generally fiber lasers offer ultrashort pulses with longer pulse width and lower pulse energy compared with solid-state lasers. However, due to the advantages of fiber lasers of compact structure, simple operation, and low cost, fiber lasers are promising to be an alternative of solid-state lasers. Therefore, fiber lasers those can generate ultrashort pulses with smaller pulse width and/or larger pulse energy are continuous research focus within the past two decades<sup>[1-7]</sup>. Ultrashort pulses generated in fiber lasers are considered as a kind of “soliton” as normally the pulses can maintain their properties at a fixed position in the cavity under a steady state. Different from the pulses propagating in conventional systems, due to the intrinsic gain-loss mechanism in lasers, pulses generated in fiber lasers are generally considered as dissipative solitons (DSs)<sup>[8-9]</sup>.

Conventional fiber lasers are operated in the anomalous dispersion regime where pulse shaping automatically occurs due to the balanced interaction between the negative cavity dispersion and the fiber Kerr nonlinear effect<sup>[1-2]</sup>. Ultrashort pulses with pulse width of hundreds of femtoseconds and pulse energy of tens of pico-joules are routinely generated. Due to the cavity peak power clamping effect<sup>[10]</sup>, increasing pump power cannot unlimitedly decrease the pulse width and increase the pulse energy, instead multiple DSs are generated. To increase the pulse energy, a dispersion-managed cavity scheme is used, where a fiber with normal dispersion is sandwiched by other fibers with negative dispersion<sup>[3]</sup>. As the pulse would be stretched when the pulse propagating in the normal dispersion fiber, the effective nonlinearity accumulated is lower than that of a pulse propagates in a comparable uniform dispersion fiber laser. Thus the energy of the pulse formed in the dispersion-managed cavity can be much improved<sup>[11]</sup>. Recently, DSs are demonstrated in fiber lasers of normal cavity dispersion<sup>[4]</sup>. In the normal dispersion regime the cavity dispersion and the fiber nonlinear Kerr effect play the same role on the propagating pulse so that no inherently stable pulse can be generated if no additional auxiliary mechanism is introduced. The gain dispersion effect can play as a counterpart against the cavity dispersion and the

nonlinear Kerr effect. Hence so-called “gain-guided solitons” can be generated in normal dispersion fiber lasers<sup>[4]</sup>. As the generated pulse is heavily chirped, much energy can be accommodated in the pulse. Therefore, it is promising to obtain large-energy pulses in the fiber lasers of normal dispersion. Chong *et al.*<sup>[5,7]</sup> also achieved heavily-chirped pulses in the normal dispersive Yb-fiber lasers with the help of a purposely inserted intracavity spectral filter as the gain bandwidth of the Yb-fiber is too broad. Bale *et al.*<sup>[12]</sup> theoretically analyzed the pulse dynamics in Yb-fiber lasers with intracavity spectral filter and claimed that the pulse energy is determined by the ratio of the filter bandwidth to the gain bandwidth and the position of the output coupler in the laser cavity. Without using any physical spectral filter in the laser cavity, DS generation was demonstrated in Yb-fiber lasers that are mode-locked by using the nonlinear polarization rotation technique<sup>[13-14]</sup>, for which the spectral filtering is realized with the birefringent filter caused by the combined effect of the polarizer and the cavity birefringence. As the doping of the Yb ions in Yb-fibers could be much larger than that of Er-fibers, which means that the gain provided by the Yb-fiber could be much stronger than that of the Er-fiber, Yb-fiber lasers are the focus for the large energy pulse source. Apart from the operation wavelength, the main difference between the Yb-fiber and the Er-fiber is the gain amplitude and the gain bandwidth, for example, the gain bandwidth of Yb-fiber is about 40 nm, far broader than that of the Er-fiber of about 20 nm. Then an interesting question immediately appears: is it possible to generate ultrashort pulses with large pulse energy in Yb-fiber lasers without using any spectral filter apart from the gain dispersion (gain bandwidth limitation)? In other words, could the broad gain bandwidth alone support the generation of the large-energy ultrashort pulses in Yb-fiber lasers? In this paper we numerically simulate the transient process of DS generation in fiber lasers of normal dispersion. We only consider the role of the spectral filtering caused by the gain bandwidth and find that it is possible to achieve pulses under broad gain bandwidth. The numerical results obtained suggest that it is promising to obtain large-energy pulse in fiber lasers of normal dispersion and broad gain bandwidth without using any other

spectral filter in the cavity. Narrow gain bandwidth results in multiple DS while broad gain bandwidth (up to 100 nm) supports DS formation if enough pump power is available. The formation of characteristic steep spectral edges of DS is also numerically elucidated.

## 2 Numerical simulations

Figure 1 shows a simplified typical fiber laser. All the fibers including the gain fiber and the single mode fibers (SMFs) have normal dispersion. We used the nonlinear polarization rotation technique<sup>[10]</sup> to achieve mode locking in the fiber laser. Therefore, the mode locker is physically equalized as a combiner of a polarization controller, a polarizer, and an isolator in the fiber laser.

The pulse tracing technique is used to simulate the pulse evolution in the fiber laser<sup>[10]</sup>. In summary, we start the simulation with an arbitrary pulse and circulate it in the laser cavity until a steady pulse evolution state

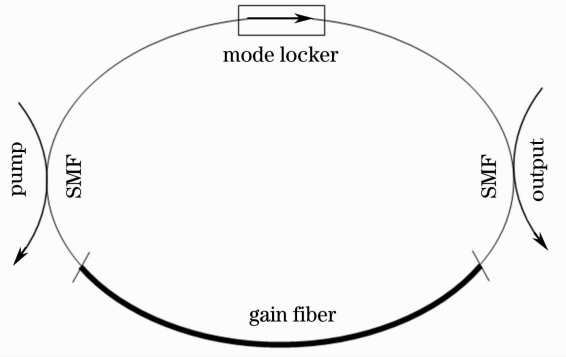


Fig.1 Schematic of the fiber laser

is established. The criterion for stable mode locking is that the output pulse energy difference between the neighboring roundtrip is less than  $10^{-3}$  pJ. Whenever the pulse encounters an individual intracavity component except the fiber segments, we multiply the Jones matrix of the component to the optical field of the pulse. The pulse propagation in the fibers is described by the coupled Ginzburg-Landau equations:

$$\begin{cases} \frac{\partial u}{\partial z} = -i\beta u + \delta \frac{\partial u}{\partial t} - \frac{ik''}{2} \frac{\partial^2 u}{\partial t^2} + \frac{ik'''}{6} \frac{\partial^3 u}{\partial t^3} + i\gamma \left( |u|^2 + \frac{2}{3} |v|^2 \right) u + \frac{i\gamma}{3} v^2 u^* + \frac{g}{2} u + \frac{g}{2\Omega_g} \frac{\partial^2 u}{\partial t^2} \\ \frac{\partial v}{\partial z} = i\beta v - \delta \frac{\partial v}{\partial t} - \frac{ik''}{2} \frac{\partial^2 v}{\partial t^2} + \frac{ik'''}{6} \frac{\partial^3 v}{\partial t^3} + i\gamma \left( |v|^2 + \frac{2}{3} |u|^2 \right) v + \frac{i\gamma}{3} u^2 v^* + \frac{g}{2} v + \frac{g}{2\Omega_g} \frac{\partial^2 v}{\partial t^2} \end{cases}, \quad (1)$$

where  $u$  and  $v$  are the normalized envelopes of the optical pulses along the two orthogonal polarization axes of the fiber,  $u^*$  and  $v^*$  are the conjugates of  $u$  and  $v$ .  $2\beta = 2\pi\Delta n/\lambda$  is the wave-number difference between the two polarization modes of the fiber, where  $\Delta n$  is the difference between the effective indices of the two modes,  $\lambda$  is the wavelength.  $2\delta = 2\beta\lambda/(2\pi c)$  is the inverse group velocity difference, where  $c$  is the light speed.  $k''$  is the second order dispersion coefficient,  $k'''$  is the third order dispersion coefficient and  $\gamma$  represents the nonlinearity of the fiber.  $g$  is the saturable gain of the fiber and  $\Omega_g$  is the bandwidth of the laser gain. For SMF,  $g = 0$ ; for the gain fiber, we considered the gain saturation as

$$g = G \exp \left[ - \frac{\int (|u|^2 + |v|^2) dt}{E_{\text{sat}}} \right], \quad (2)$$

where  $G$  is the small-signal-gain coefficient and  $E_{\text{sat}}$  is the normalized saturation energy.

Different from previous research<sup>[4,7,10,12-13]</sup> where only the final steady state is concerned, here we focus

on the transient process of DS generation. The purpose of the numerical simulations is to reveal the transient process that how the initial arbitrary pulse evolves into stable DS under the combined interaction among cavity dispersion, fiber nonlinearity, laser gain and loss, and spectral filtering caused by the gain dispersion. Therefore, the operation parameters are so selected that the DSs can be fast achieved within tens of roundtrip calculation. To exclude the influence of the birefringent filter caused by the polarizer and the cavity birefringence<sup>[13]</sup>, we choose  $L/L_b = 2$  ( $L_b$  is the beat length and  $L$  is the cavity length), which makes the width of the birefringent filter to be larger than 200 nm.

We use the dispersion parameters of the Yb-fiber laser in Ref. [7], the definition of the parameters could be found in Ref. [10]. The parameters are summarized in Table 1.  $L = 3$  m (SMF) + 0.6 m (gain fiber) + 1 m (SMF) = 4.6 m. The output position is in the middle of the last segment of SMF and 10% output is taken into account.

Table 1 Parameters used in the simulations

| Parameter  | Value      |
|--|------------|
| $\gamma / (\text{W}^{-1} \cdot \text{km}^{-1})$        | 3          |
| $k''_{\text{SMF}} / (\text{ps}^2 / \text{km})$         | 23         |
| $L / L_b$  | 2          |
| $\phi / \text{rad}$                                    | $0.652\pi$ |
| $k''_{\text{gain, fiber}} / (\text{ps}^2 / \text{km})$ | 13         |
| $k''' / (\text{ps}^3 / \text{km})$                     | -0.13      |
| $\theta / \text{rad}$                                  | $0.152\pi$ |
| $P_{\text{sat}} / \text{nJ}$                           | 2          |

Figures 2 (a) and (b) show the temporal profiles and the optical spectra of the generated DSs. To obtain the states, all the parameters are fixed except the gain bandwidth. We started from a same small arbitrary pulse. The cavity linear phase delay bias (CLPDB)<sup>[10]</sup> is set at  $1.7\pi$  and the small signal gain is  $G = 5000 \text{ km}^{-1}$ . Similar to the results obtained in Er-fiber lasers<sup>[4]</sup>, narrow gain bandwidth can support the DS. However, it is found that DS can be achieved even when the gain bandwidth is chosen to be 100 nm, which is far larger than the real gain bandwidth of Yb-fiber. Figures 2(c) and (d) show the pulse profile and the chirp for two cases: gain bandwidth is 20 nm and 100 nm, respectively. The linear chirp over the

pulse profile suggests that it is compressible. The pulse obtained when the gain bandwidth is 100 nm is broader than the pulse observed when the gain bandwidth is 20 nm. It is out of our expectation that such a broad gain bandwidth (100 nm) alone can still support the DS generation. From the performance of the generated DS when the gain bandwidth is changed from 10 nm to 50 nm, we can find that the pulse width increases with the increasing gain bandwidth while the spectral bandwidth reduces. Therefore, a gain medium with broader gain bandwidth is better for large energy pulse generation as wider pulse can lower the peak power, consequently reduce nonlinearity, and hence accommodate more energy in the chirped pulses. Figure 3 shows, for example, the pulse energy of stable pulse at the 10% output versus different gain bandwidth when the CLPDB is fixed at  $1.7\pi$  and the small signal gain is  $G = 3.2 \times 10^5 \text{ km}^{-1}$ . It is obvious that broader gain bandwidth can support larger pulse energy. We note that the pulse energy under gain bandwidth of 100 nm could be further increased with larger small-signal-gain

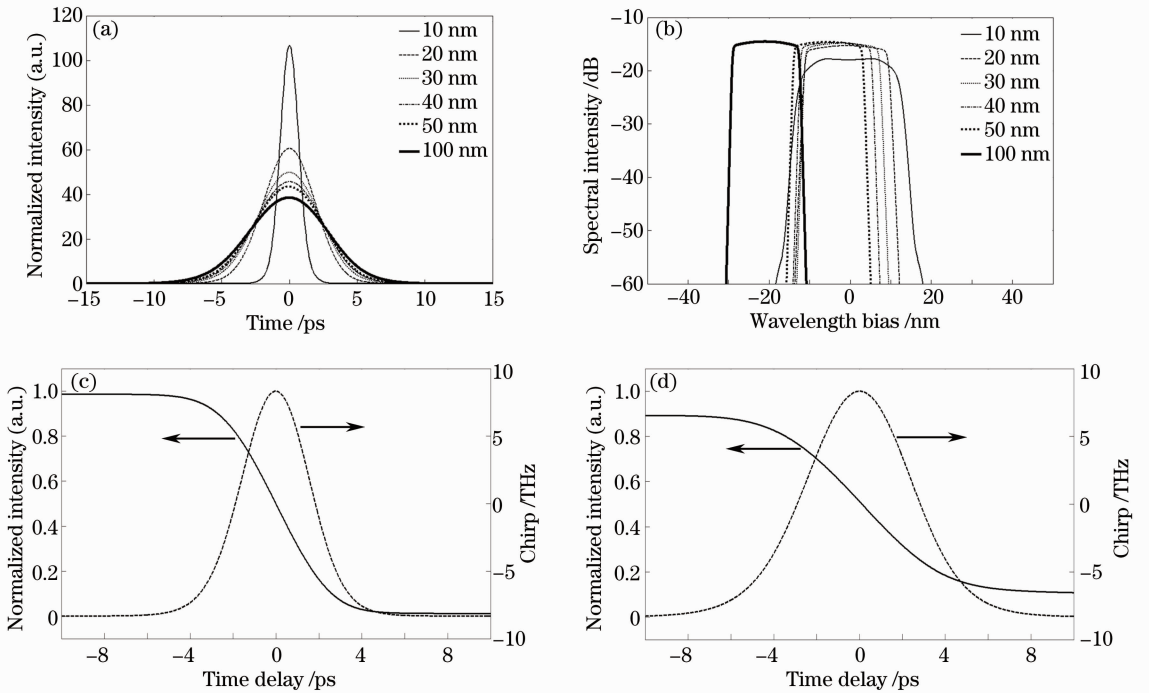


Fig.2 (a) Pulse profiles and (b) spectra of dissipative solitons with different gain bandwidths (CLPDB is  $1.7\pi$  and  $G = 5000 \text{ km}^{-1}$ , central wavelength is 1064 nm); stable pulse profile and chirp when gain bandwidth is (c) 20nm and (d) 100 nm, respectively

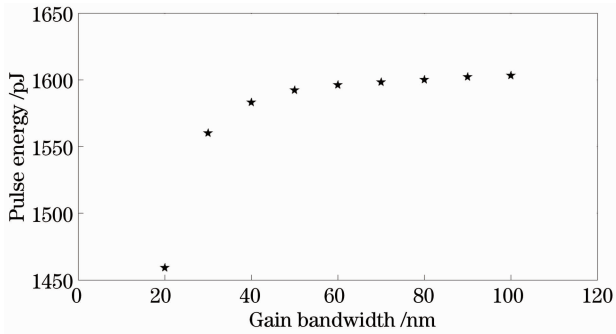


Fig.3 Pulse energy versus gain bandwidth when the CLPDB is fixed at  $1.7\pi$  and the small-signal-gain is  $G = 3.2 \times 10^5 \text{ km}^{-1}$

(stronger pump power) until the appearance of multiple pulsing or period doubling. It is desired to know how the broad gain bandwidth (100 nm) support the DS generation.

Figure 4 shows the optical spectra of the transient pulse at two positions, one is before and the other is after the gain fiber, in the first roundtrip and the 50th roundtrip, respectively. The corresponding videos<sup>[15]</sup> show the transient process that how a DS is generated from a small arbitrary pulse. Typical result is shown in Video A<sup>[15]</sup> for the case that the gain bandwidth is 20 nm. It is clear that due to the narrow gain bandwidth the transient pulse is amplified and simultaneously spectrally shaped until the stable DS is generated. We note that the video shows the lumped change of the transient pulse every roundtrip. At the first stage (roundtrip, 1 ~ 6), the small arbitrary pulse is amplified. As the pulse is so weak, its spectrum is so narrow that the gain dispersion effect is not significant and the pulse as a whole is amplified. Figure 5(a) shows the pulse spectrum at roundtrip 6. Then from the 7th roundtrip, as the spectral peak of the transient pulse is so high that the nonlinear phase shift is so large that the cavity transmission for this spectral component is reduced, consequently the dynamic loss is larger than the dynamic gain for this spectral component. In other words, the spectral peak of the transient pulse cannot be unlimitedly amplified. Hence, a spectral dip (roundtrip 7) appears at the position of the original spectral peak (roundtrip 6), as shown

in Figure 5(b). The dip further develops as shown in Figure 5(c) (roundtrip 8) while the whole spectrum is broadened. If the spectral intensity of a certain spectral component is so low that the nonlinear phase shift is reduced that the cavity transmission increases again, the spectral component can be amplified again, which is elucidated by the change from roundtrip 8 to roundtrip 9 where the dip spectral center is transformed into peak spectral center again, as shown in Figure 5(d). Therefore, there exists a peak clamping effect in the spectral domain that is determined by the cavity transmission curve, which is determined by the CLPDB and the cavity birefringence<sup>[16]</sup>. As the spectral component in the center of the spectrum is amplified and clamped firstly, the spectral components near the spectral center of the transient pulse will then be amplified until they are clamped as well. This process gradually extends to the both sides of the spectrum, as shown in Figure 5. At the same time, due to the gain dispersion or the gain bandwidth limitation, the spectral components of the transient pulse located out of the 3 dB gain bandwidth range experience a much larger dynamic loss during the transient amplification process. Then, once the balance between the dynamic gain and dynamic loss under the gain bandwidth limitation is achieved, a DS is generated as shown in Video A<sup>[15]</sup>. Hence, the characteristically steep spectral edges of the generated DS are indeed caused by the gain dispersion. And the top structure of the spectrum of the DS is determined by the detailed gain profile and the cavity transmission. Seeing from another side, the fiber nonlinearity expands the spectrum of the propagating pulse while it is amplified during propagation, meanwhile the normal cavity dispersion introduces the positive chirp. Due to the gain dispersion effect, the gain imposed on the propagating pulse is wavelength dependent. Only when the dynamic gain affecting on a certain spectral component is larger than the dynamic loss, the spectral component will be amplified. Independent of the detailed gain profile, the gain

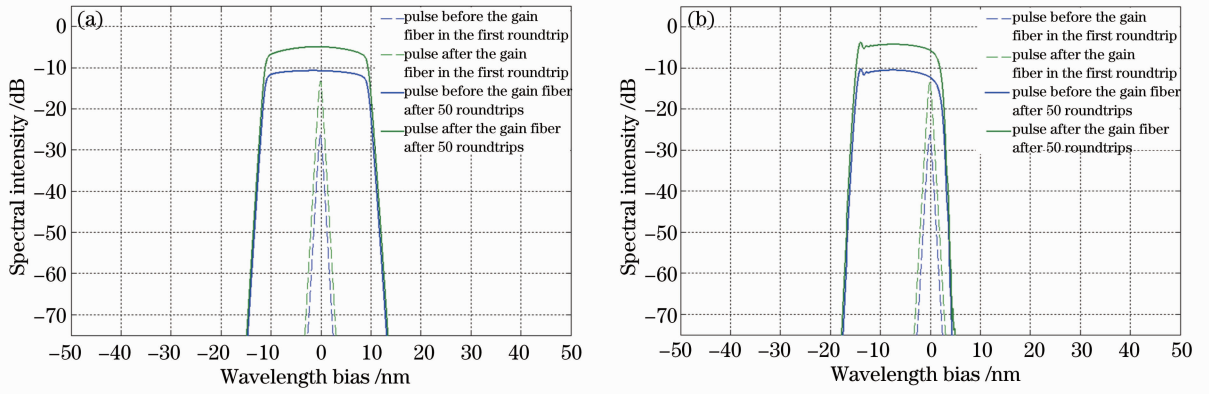


Fig. 4 Optical spectra of the transient pulse at different intracavity positions during evolution when gain bandwidths are (a) 20 nm and (b) 100 nm, central wavelength is 1064 nm

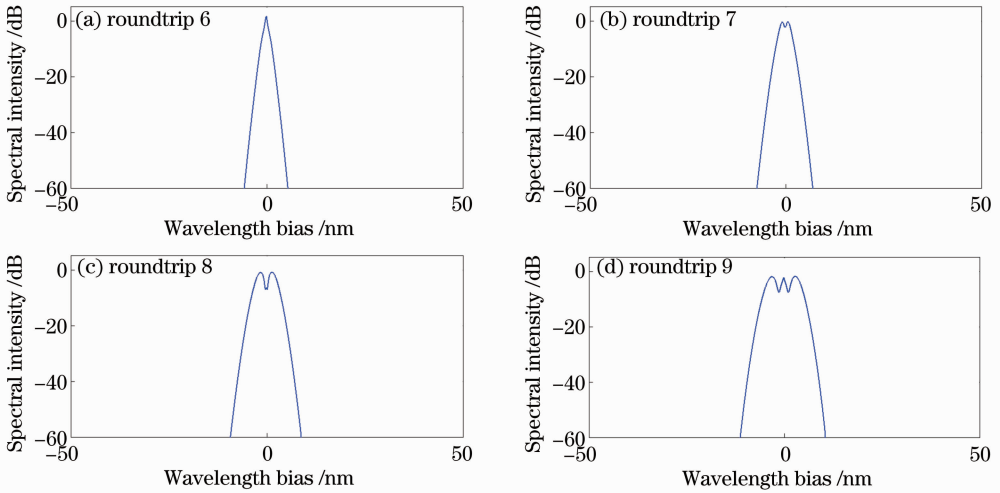


Fig. 5 Optical spectra of the transient pulse at different roundtrips when gain bandwidth is 20 nm, central wavelength is 1064 nm

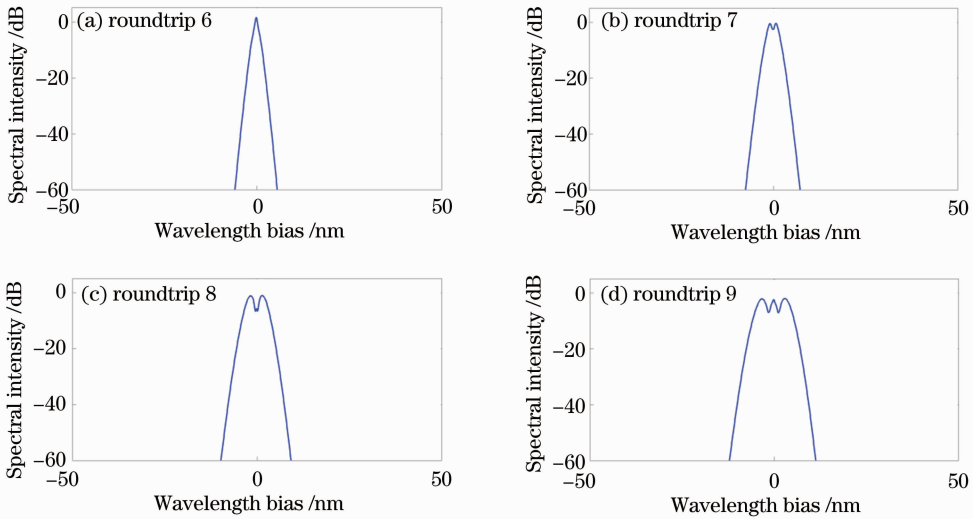


Fig. 6 Optical spectra of the transient pulse at different roundtrips when gain bandwidth is 100 nm, central wavelength is 1064 nm

profile always declines away from its center. In other words, there always exist two watersheds away from the gain center where the dynamic loss dominates the dynamic gain. Therefore, steep spectral edges are ultimately formed under the combined interaction among the normal dispersion, fiber nonlinearity, gain and loss, and gain dispersion effects.

Video B<sup>[15]</sup> shows the pulse evolution when the gain bandwidth is 100 nm. We can see that there are two main developing stages; the first one is similar to Video A<sup>[15]</sup>, where a transient pulse with steep spectral edges is generated from a same small arbitrary pulse; the second one is the shifting of the whole spectrum accompanying with tiny spectrum shaping. Figure 6 shows the first stage of the spectrum evolution when gain bandwidth is 100 nm. There is similar spectrum clamp effect as shown in Figure 5. Different from the narrow gain bandwidth case of Video A<sup>[5]</sup>, the spectrum of the transient pulse continuously shifts until it reaches and stabilizes at one wing within the gain bandwidth regime as shown in Figure 2(b), which is caused by the wavelength offset between the gain profile and the birefringence filter resulting from the nonlinear polarization rotation technique<sup>[13]</sup>.

From the two videos, we know that the gain dispersion effect plays its role from the beginning of the pulse evolution. It always trims off the spectral component far away from the center of the gain profile. During the pulse amplification, the dynamic balance between the effective gain and effective loss within the gain bandwidth will ultimately determine the finally generated DS.

Numerically we confirmed that when the gain bandwidth is narrow and the pump power is strong enough, multiple DS would be generated, which has been demonstrated in Er-fiber lasers<sup>[17]</sup> and Yb-fiber lasers<sup>[18]</sup>. Practically each individual component in the fiber laser such as the wavelength-division-multiplexing coupler, the output coupler, or the polarizer, has its own bandwidth, which will help to change the effective bandwidth of spectral filter in the cavity.

Therefore, the detailed spectral filtering in the fiber laser is dynamically determined by each component's bandwidth and the gain bandwidth. As we can numerically obtain DS in fiber lasers those only the broad gain bandwidth limitation (up to 100 nm) is considered, it is no doubt that DS can be achieved in Yb-fiber lasers whose gain bandwidth is normally around 40 nm, and no discrete spectral filter is required in these fiber lasers.

### 3 Conclusion

In conclusion, the transient process of DS generation in normal dispersion fiber lasers is numerically explored. The physical mechanism of the formation of the steep spectral edges of DS is explained. DS are numerically demonstrated in normal dispersive fiber lasers with gain bandwidth as broad as 100 nm and without considering any other spectral filtering effect in the fiber lasers. The numerical results suggest that it is promising to generate large energy pulse in normal dispersion fiber lasers with broad gain bandwidth and without using any discrete spectral filter in the laser cavity.

### References

- 1 D J Richardson, R I Laming, D N Payne, *et al.*. 320 fs soliton generation with passively mode-locked erbium fibre laser [J]. *Electron Lett*, 1991, 27(9): 730 – 732.
- 2 S M J Kelly, K Smith, K J Blow, N J Doran. Average soliton dynamics of a high-gain erbium fiber laser [J]. *Opt Lett*, 1991, 16 (17): 1337 – 1339.
- 3 K Tamura, E P Ippen, H A Haus, *et al.*. 77-fs pulse generation from a stretched-pulse mode-locked all-fiber ring laser [J]. *Opt Lett*, 1993, 18(13): 1080 – 1082.
- 4 L M Zhao, D Y Tang, J Wu. Gain-guided soliton in a positive group dispersion fiber laser [J]. *Opt Lett*, 2006, 31(12): 1788 – 1790.
- 5 Andy Chong, Joel Buckley, Will Renninger, *et al.*. All-normal-dispersion femtosecond fiber laser [J]. *Opt Express*, 2006, 14 (21): 10095 – 10100.
- 6 L M Zhao, D Y Tang, T H Cheng, *et al.*. Ultrashort pulse generation in lasers by nonlinear pulse amplification and compression [J]. *Appl Phys Lett*, 2007, 90(5): 051102.
- 7 A Chong, W H Renninger, F W Wise. Properties of normal-dispersion femtosecond fiber lasers [J]. *J Opt Soc Am B*, 2008, 25 (1): 140 – 148.
- 8 N Akhmediev, A Ankiewicz. (eds.) *Dissipative Solitons Vol. 18, Lecture Notes in Physics, Vol. 661* [M]. Heidelberg: Springer.

- 2005.
- 9 N Akhmediev, A Ankiewicz. (eds.) Dissipative Solitons: From Optics to Biology and Medicine, Lecture Notes in Physics, Vol. 751 [M]. Heidelberg: Springer, 2008.
- 10 D Y Tang, L M Zhao, B Zhao, *et al.*. Mechanism of multisoliton formation and soliton energy quantization in passively mode-locked fiber lasers [J]. Phys Rev A, 2005, 72(4): 043816.
- 11 N J Smith, F M Knox, N J Doran, *et al.*. Enhanced power solitons in optical fibres with periodic dispersion management [J]. Electron Lett, 1996, 32(1): 54 – 55.
- 12 Brandon G Bale, J Nathan Kutz, Andy Chong, *et al.*. Spectral filtering for mode locking in the normal dispersive regime [J]. Opt Lett, 2008, 33(9): 941 – 943.
- 13 Luming Zhao, Dingyuan Tang, Xuan Wu, *et al.*. Dissipative soliton generation in Yb-fiber laser with an invisible intracavity bandpass filter [J]. Opt Lett, 2010, 35(16): 2756 – 2758.
- 14 Zuxing Zhang, Guoxing Dai. All-normal-dispersion dissipative soliton ytterbium fiber laser without dispersion compensation and additional filter [J]. IEEE Photonics Journal, 2011, 3(6): 1023 – 1029.
- 15 [http://v.youku.com/v\\_show/id\\_XNTk5MZE0NTky.html](http://v.youku.com/v_show/id_XNTk5MZE0NTky.html);  
[http://v.youku.com/v\\_show/id\\_XNTk5MZEW0TAW.html](http://v.youku.com/v_show/id_XNTk5MZEW0TAW.html).
- 16 W S Man, H Y Tam, M S Demokan, *et al.*. Mechanism of intrinsic wavelength tuning and sideband asymmetry in a passively mode-locked soliton fiber ring laser [J]. J Opt Soc Am B, 2000, 17(1): 28 – 33.
- 17 L M Zhao, D Y Tang, T H Cheng, *et al.*. Generation of multiple gain-guided solitons in a fiber laser [J]. Opt Lett, 2007, 32(11): 1581 – 1583.
- 18 Janet W Lou, Marc Currie, Fredrik K Fatemi. Experimental measurements of solitary pulse characteristics from an all-normal-dispersion Yb-doped fiber laser [J]. Opt Express, 2007, 15(8): 4960 – 4965.

栏目编辑: 张 腾